Multiple scattering effects due to hydrometeors on precipitation radar systems

Multiple scattering effects due to hydrometeors on precipitation radar systems

A. Battaglia
Meteorological Institute, University of Bonn, Bonn, Germany

M. O. Ajewole
Department of Physics, Federal University of Technology, Akure, Nigeria

C. Simmer
Meteorological Institute, University of Bonn, Bonn, Germany

Received 15 June 2005; revised 13 July 2005; accepted 31 August 2005; published 4 October 2005.

[1] Space-borne radars are invaluable tools for characterizing clouds and precipitation. At higher frequencies (like those used for the TRMM PR or envisaged for GPM radars) attenuation due to hydrometeors increasingly becomes a relevant issue. Simultaneously when dealing with active sensors, multiple scattering effects could be significant due to the simultaneous increase of the optical thickness and the single scattering albedo of the hydrometeors with frequency. In this study, we investigate multiple scattering due to rainfall and graupel on radar returns for nadir observations at 13 and 35 GHz. A numerical approach, based on the forward fully polarized Monte Carlo technique, which incorporates a Gaussian antenna pattern function with varying beamwidths, is adopted in the study. Results reveal that multiple scattering effects are driven by the interplay between the antenna footprint, the medium scattering coefficient and the depth traveled inside the medium. The multiple scattering effects are generally negligible at 13 GHz for typical space-borne and air-borne systems while they are relevant to space-borne but almost negligible in air-borne configurations at 35 GHz. **Citation:** Battaglia, A., M. O. Ajewole, and C. Simmer (2005), Multiple scattering effects due to hydrometeors on precipitation radar systems, *Geophys. Res. Lett.*, *32*, L19801, doi:10.1029/2005GL023810.

1. Introduction

[2] Space-borne radars are invaluable tools for characterizing clouds and precipitation as demonstrated by the tropical rainfall measuring mission (TRMM) precipitation radar. Higher frequency space-borne radars are being envisaged for up-coming missions such as the 35.5 GHz precipitation radar on-board the global precipitation mission (GPM) satellite and its European version (EGPM).

[3] Radar measurements are often interpreted assuming the absence of multiple scattering (MS). Considering satellite missions using high-frequency radars, it is necessary to evaluate the correctness of this assumption. In the millimeter region, the scattering and absorption cross sections of raindrops are comparable: this increases considerably the probability of scattering versus absorption events. Moreover, the larger the size parameter the more peaked is the scattering phase function in the forward direction: this will increase the probability of the scattered photons to remain inside the field of view of the instrument.

[4] The multiple-scattering phenomenon in active remote sensing has been extensively studied by the lidar community [see *Bissonnette et al.*, 1995]. For lidars the effect is aggravated by the strongly peaked phase function typical of ice/water particles in the optical scattering regime. Radars have generally larger fields of view than lidars (2–20 mrad compared to 0.1–5 mrad for lidars). This should enhance the MS effect. On the other hand, at radar frequencies, phase functions are not as much peaked as in the visible or near infrared region, and clouds are less efficient scatterers. Since noticeable multiple-scattering effects are expected in optically thick regions, they are likely to be present in regions of strong attenuation as well. Attenuation is particularly important for ground based radars at frequencies in and above the *X*-band and for space-borne radars at frequencies in and above K_a–band. Thus in heavy rain, reflectivity information can be completely lost from large portions of a radar scan. In this paper we assess whether or not MS effects, when present, are actually detectable [i.e., higher than detection thresholds (DT)].

[5] MS effects have been extensively evaluated for passive microwave link applications [see *Ishimaru et al.*, 1982; *Ajewole and Oguchi*, 2004]. Only few authors [*Oguchi et al.*, 1994; *Ito et al.*, 1995; *Marzano et al.*, 2003] have, however, investigated MS effects on radar-based rainfall estimates. These studies concluded that the difference between single and MS signals is significant, especially for heavy rain cases. In particular, *Marzano et al.* [2003] show that, in the presence of strongly attenuating media, MS contributions enhance the detection of the signal by partly overcoming the apparent path attenuation. This finding has an immediate impact on rainfall retrieval algorithms like the dual-wavelength methods based on the surface reference techniques [e.g., *Testud et al.*, 1992]. Both *Oguchi et al.* [1994] and *Marzano et al.* [2003] did, however, not account for the effect of the antenna pattern. *Oguchi et al.* [1994] cautioned that "MS calculations based on plane wave incidence may overestimate the effect of multiple scattering, since the scattered wave generated by the plane-wave illuminated drops far from the receiver antenna beam may contribute

0094-8276/05/2005GL023810$05.00

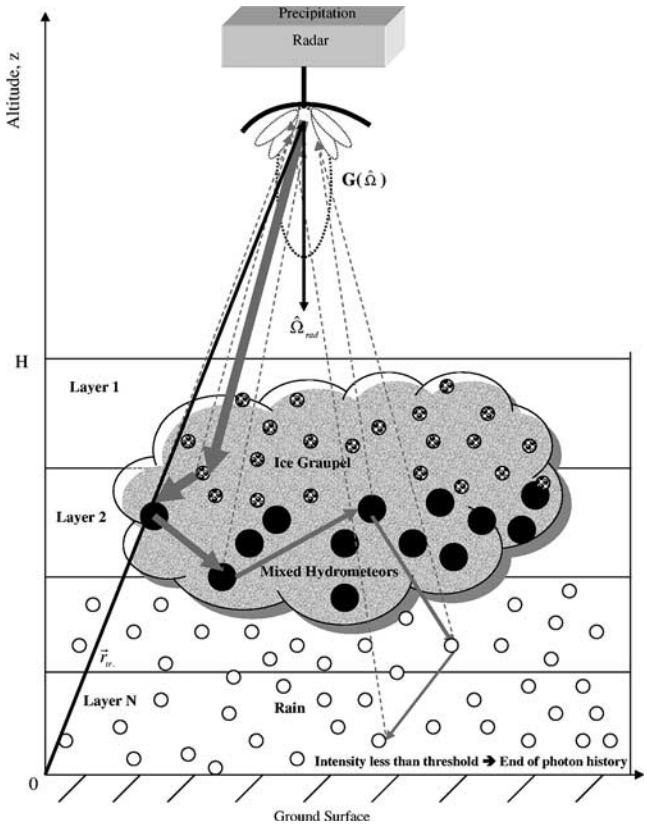

Figure 1. Geometry and principles of forward Monte Carlo algorithm to compute the MS apparent reflectivity Z_a^{MS} for a monostatic radar ($\vec{\mathbf{r}}_{tr.} = \vec{\mathbf{r}}_{rec.}$).

to the received incoherent power through successive scattering.'' Similarly, *Marzano et al.* [2003] did not include any antenna beam-width effect. Although *Marzano et al.*'s [2003] Figure 1 depicted an antenna pattern, they did not take it into account in their simulations. In addition, the microwave ''photons'' are traced back in the direction of the incident plane wave and not towards the true location of the radar receiving antenna. These omissions lead to an enormous MS effect at 35 GHz (as shown by *Marzano et al.* [2003, Figure 4 [right]]), which could compensate for the strong attenuation due to intense/heavy rain. Their results would practically allow the detection of a heavy rain column event with a 35 GHz space-borne radar (like those planned for GPM or EGPM).

[6] MS effects are strongly dependent on the field of view of the instruments; for instance a pencil beam will not suffer any MS effect. It is thus the main purpose of this paper to provide a realistic estimate of the multiple scattering effect expected from typical radars with frequencies higher than 10 GHz by taking into account the actual distances of the radar from the rain layer and that radars have antenna beam-width usually less than 1°.

2. The Radar Equation in the Presence of MS: Theoretical Background and Numerical Implementation

[7] The classical radar equation [e.g., see *Bringi and Chandrasekar*, 2001] usually provides the apparent reflectivity as a function of single scattering (SS) contributions only. It is usually written as

$$\langle P_{aR}(r)\rangle = \frac{A_{e0}G_0\Omega_{2A}\Delta r}{(4\pi)^2}\frac{\pi^5|K|^2}{\lambda^4}\frac{P_T}{r^2}\,Z_a^{SS} \tag{1}$$

where λ is the wavelength, P_T is the transmitted power, Δr is the range resolution, $G_0 = \dfrac{4\pi}{\Omega_p}$ is the maximum directive gain ($\Omega_p = \int F_n(\hat{\mathbf{\Omega}})\, d\Omega$ is the antenna pattern solid angle), $A_{e0} = \frac{\lambda^2 G_0}{4\pi}$, Ω_{2A} is the two way main-lobe solid angle and Z_a^{SS} is the SS apparent radar reflectivity at range r, which is related to the equivalent reflectivity factor Z_e by

$$Z_a^{SS}(r) \equiv \underbrace{\left[\frac{\lambda^4}{\pi^5|K|^2}\int_D \sigma_{back}(D)N(D)dD\right]}_{Z_e(r)}\; e^{-2\int_o^r k_{ext}(\xi)\,d\xi}$$

with $|K|^2$, σ_{back}, k_{ext} and $N(D)$ the dielectric factor, the backscattering cross section, the extinction coefficient and the size distribution of the scatterers inside the radar backscattering volume, respectively. In the simulations we will always normalize the dielectric factor to that of water at $T = 0$°C (i.e., 0.93 for all frequencies considered hereafter).

[8] On the other hand the apparent (or effectively measured) back-scattered received power from a range gate at distance r in the presence of MS can be generally expressed as [*Tsang et al.*, 1985]:

$$\langle P_{aR}(r)\rangle = \frac{\lambda^2}{4\pi}\int_{4\pi} G\left(\hat{\mathbf{\Omega}}'\right)\langle I_{aR}\left(r,\hat{\mathbf{\Omega}}'\right)\rangle d\Omega' \tag{2}$$

where $\langle I_{a\ R}(r,\ \hat{\mathbf{\Omega}}')\rangle$ is the mean value of the apparent received specific intensity, $G(\hat{\mathbf{\Omega}}) = G_0F_n(\hat{\mathbf{\Omega}})$ is the antenna gain and $F_n(\hat{\mathbf{\Omega}})$ is the normalized (in the sense that the maximum is equal to 1) antenna pattern (equal to the squared modulus of the antenna field pattern).

[9] By comparing (2) and (1) we can define the apparent MS reflectivity by:

$$Z_a^{\mathrm{MS}} \equiv \left[\frac{\int_{4\pi} F_n\left(\hat{\mathbf{\Omega}}'\right)\langle I_{aR}\left(r,\hat{\mathbf{\Omega}}'\right)\rangle r^2 d\Omega'}{P_T}\right]\frac{\lambda^4}{\pi^5|K|^2}\frac{(4\pi)^2}{G_0\Omega_{2A}\Delta r} \tag{3}$$

Obviously Z_a^{SS} ($\leq Z_a^{\mathrm{MS}}$) can be computed using (3) by considering only the single-scattering contributions in $I_{a\ R}$. To compute the apparent MS reflectivity defined by (3) it is necessary to evaluate the received specific intensity from all relevant scattering orders, as depicted in Figure 1. As by *Marzano et al.* [2003], we have solved the radiative transfer equation using a Monte Carlo solution technique, that adopts biasing techniques. Instead of using backward Monte Carlo technique we have modified the forward Monte Carlo technique by *Battaglia and Mantovani* [2005]. In the case of an active sensor response simulation, the backward approach has no computational advantage since the only source of photons is the radar. The Monte Carlo technique was adopted in this study because of its flexibility in simulating 3D-structured clouds and the antenna pattern and position.

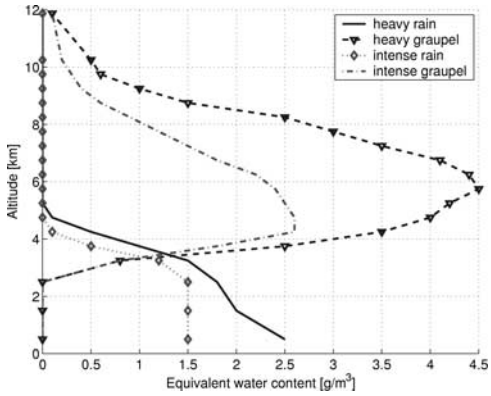

Figure 2. Equivalent water content vertical profiles of rain and graupel for intense and heavy precipitation.

[10] The forward Monte Carlo code has been modified to simulate the active sensor response by keeping track of the distance traveled by each photon and by allowing the radar to be the only source of radiation. In our code the radar is characterized by:

[11] • a localized transmitting $\vec{\mathbf{r}}_{tr.}$ and receiving position $\vec{\mathbf{r}}_{rec.}$ (to allow for bistatic antenna configurations), including the satellite altitude H_{sat} (in case of space-borne configurations);

[12] • a pointing solid angle $\hat{\Omega}_{rad.}$, or equivalently by two angles ($\Theta_{rad.}$, $\Phi_{rad.}$);

[13] • a Gaussian antenna pattern function $F_n(\hat{\mathbf{\Omega}})$:

$$F_n(\eta,\xi) = e^{-4\log(2)\left[\frac{\eta^2}{\theta^2_{3dB}}+\frac{\xi^2}{\phi^2_{3dB}}\right]} \tag{4}$$

where η and ξ are the angles in the $E-$ and $H-$ antenna plane while θ_{3dB} and ϕ_{3dB} are the beam-widths at 3 dB.

[14] • an emitting and a receiving polarization state;

[15] • a range resolution $\Delta r = c\Delta t/2$, with Δt the pulse duration.

[16] The radar outgoing radiation is simulated by N_T photons per unit time, with N_T high enough to represent the stochastic variability of all processes involved in photon propagation and interactions when released from the transmitting radar antenna with an appropriate polarization state. Each photon carries a unit energy while the angular distribution function is that provided by the Gaussian antenna pattern.

[17] All stochastic processes are simulated as in the Monte Carlo version for passive sensors and the associated Stokes vector are properly modified. Each time a scattering event happens at point $\vec{\mathbf{r}}_{sc}$, the apparent range bin is first computed. Then the contributions to the Stokes vector received by the radar from a particular range bin (i.e., ranges between $r - \Delta r/2$ and $r + \Delta r/2$) for all N_T photons are summed up and averaged:

$$\sum^{N_T,\,N_s} \frac{F_n\left(\hat{\mathbf{\Omega}}_v\right)P(\vec{\mathbf{r}}_{sc} \rightarrow \vec{\mathbf{r}}_{rec.})S\left(\vec{\mathbf{r}}_{sc};\hat{\mathbf{\Omega}}_i,\hat{\mathbf{\Omega}}_v\right)\bar{I}(\vec{\mathbf{r}}_{sc};N_s)}{N_T} \tag{5}$$

with N_s being the scattering order. S represents the normalized phase matrix of the medium at $\vec{\mathbf{r}}_{sc}$ relative to the incoming direction $\hat{\mathbf{\Omega}}_i$ of the photon before the N_s order scattering, and the scattered direction $\hat{\mathbf{\Omega}}_v$ toward the receiving antenna. In (5) $F_n(\hat{\mathbf{\Omega}}_v)$ is a scalar term which takes into account the antenna pattern in the receiving segment and $P(\vec{\mathbf{r}}_{sc} \rightarrow \vec{\mathbf{r}}_{rec.})$ is the 4×4 propagation matrix [see *Battaglia and Mantovani*, 2005]. Equation (5) represents the statistical Monte Carlo counterparts of the non-dimensional term inside the square parenthesis on the right side of formula (3) with the only difference that it includes the four Stokes components.

3. Numerical Results

[18] For our computations we had in mind the TRMM PR radar, the dual wavelength PR and the 35 GHz radars envisaged for GPM and EGPM missions covering satellite altitudes from 350 km (TRMM) to 650 km (EGPM). Gaussian beam-widths range from $\theta_{3\ dB} = \phi_{3\ dB} = 0.71°$ for TRMM PR to 0.5° for the radar on EGPM, leading to horizontal resolutions around 4 to 6 km. On the other hand airborne radar systems typically operate with footprints of the order of 100 m. We reproduced the two profiles of intense and heavy convective precipitation shown by *Marzano et al.* [2003] (see Figure 2) corresponding to 30 and 50 mm/h rain-rate, respectively. The hydrometeor size distributions and densities were also chosen analogous to *Marzano et al.* [2003]. The SS albedo, the equivalent reflectivity and the one-way path attenuation profiles are quite similar to those shown in Figures 2–3 by *Marzano et al.* [2003]. As an order of magnitude the optical thickness of the heavy convective rain medium is 1.8 and 9.9 while for the graupel 0.15 and 4.5 at 13 and 35 GHz respectively. The mean photon path can decrease down to 1.6 km (300 m) in the heavy rain portion and to 16 km (1 km) at the graupel maximum density level at 13 GHz (35 GHz). Figures 3–4 are the single and multiple scattering reflectivity profiles at different horizontal resolutions; the diamond curves correspond to airborne configurations, the crosses to spaceborne while the triangular line to a computation procedure similar to that adopted for Figure 4 by *Marzano et al.* [2003] with an "infinite horizontal resolution". The strong attenuation

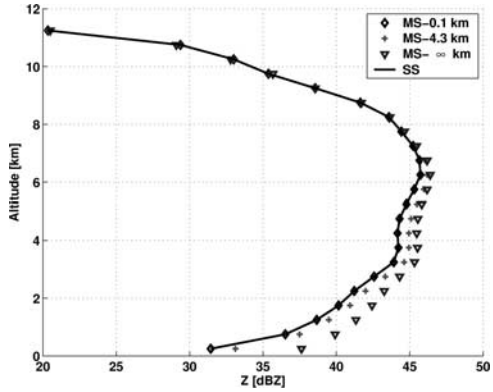

Figure 3. Apparent SS and MS reflectivity at 13.8 GHz for the heavy convective precipitation profile of Figure 2. The radar is looking downward at nadir from above the cloud system. A vertical resolution of 500 m and different horizontal resolutions are considered.

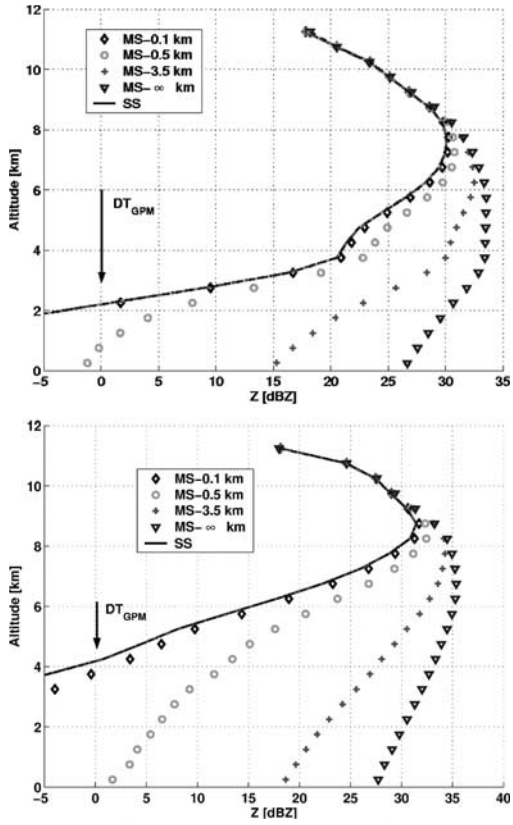

Figure 4. Same as Figure 3 at 35.5 GHz but both for (top) intense and (bottom) heavy convective precipitation.

dampens the SS signal coming from the lower layers: at 13 GHz the signal from close to the surface remains above the typical reflectivity detection threshold (10 dBZ). At 35 GHz, however, the envisaged EGPM radar (with a DT around 0 dBZ) would not detect SS signals below 4 and 2 km for the heavy and the intense precipitation profiles, respectively.

[19] The MS signal is obviously strongly dependent on the antenna horizontal resolution: what really matters is the interplay between the mean free path l, the radar horizontal resolution [obtained by the product $H_{sat}\sin(\theta_{3dB})$], the scattering layer albedo coefficient and the distance traveled inside the medium. The importance of MS effects increases with the depth traveled, and the albedo of the scattering medium, and for l much lower than the horizontal resolution.

[20] In the heavy convective profile (see Figure 3) the MS component ($Z_a^{MS} - Z_a^{SS}$) is practically absent at 13 GHz (never higher than 1.5 dB) because only rain (a 4-km thick layer) has a mean free path comparable to TRMM-like horizontal resolution, but in this region the albedo is lower than 0.17. A fortiori the intense precipitation profile (not shown) presents even less MS.

[21] On the other hand both intense and heavy reflectivity profiles, as observed by a GPM satellite-borne configuration (3.5 km line in Figure 4), are strongly affected by MS; a conclusion common to *Marzano et al.* [2003]. However in that paper the effect was overestimated (compare 3.5 km line and ∞ line) because of the absence of an antenna pattern suppression factor. A remarkable feature is represented by the fact that, when considering typical DT, MS makes the radar echo well detectable in all the heavy raining region. Vice-versa the MS signal is negligible in air-borne configuration where signals are above DT (just a little displacement of 2 dB between the SS line and the 0.1 km MS line can be seen in the bottom panel of Figure 4 in the proximity of the height of 4 km).

[22] The heavy rain profile can be considered as an extreme case because of the thickness and the amount of the rain region; as such the MS effects found here can be estimated to be the highest achievable for nadir-looking radars.

4. Discussions and Conclusions

[23] We demonstrated the necessity to take into account the antenna pattern when dealing with mm-radar MS effects. The assumption of negligible multiple scattering components is certainly valid at 13 GHz and generally applicable at 35 GHz for airborne system. Errors related to the single scattering approximation should be small when compared with other uncertainties involved in retrievals. Problems related to backscattering enhancement (that cannot be accounted for in our approach based on the radiative transfer theory [*Tsang et al.*, 1985]) that are likely only in the presence of consistent MS and for monostatic radars with small antenna aperture, are ruled out in these cases. On the other hand MS does play a very important role in typical K_a band space-borne configuration (like future GPM), at least where thick highly scattering layers are considered (like those found in convective cells). In our opinion and as a suggestion for preliminary studies of the GPM mission, airborne field campaigns should try to validate the MS effect in heavy rain scenarios by using antennas with different spatial resolutions (and lower than those actually deployed).

[24] Finally, the approach used by other authors partly overestimates MS effects when typical space-borne radar conditions are met since they practically consider infinite radar footprints. As a consequence, 1-D approaches cannot be used to solve the radiative transfer equation when MS signals are sought.

[25] **Acknowledgment.** Dr. Ajewole is grateful to the Alexander von Humboldt Foundation, to the University of Bonn and to the Federal University of Technology of Akure for the research visit to Germany.

References

Ajewole, M. O., and T. Oguchi (2004), Attenuation and depolarization of millimiter waves due to incoherent scattering in tropical rainfall, *J. Quant. Spectrosc. Radiat. Transfer*, *83*, 149–158.

Battaglia, A., and S. Mantovani (2005), Forward Montecarlo computations of fully polarized microwave radiation in non isotropic media, *J. Quant. Spectrosc. Radiat. Transfer*, *95*, 285–308.

Bissonnette, L. R., et al. (1995), Lidar multiple scattering from clouds, *Appl. Phys. B*, *60*, 355–362.

Bringi, V. N., and V. Chandrasekar (2001), *Polarimetric Doppler Weather Radar, Principles and Applications*, Cambridge Univ. Press, New York.

Ishimaru, A., R. Woo, J. Armstrong, and D. Blackman (1982), Multiple scattering calculations of rain effects, *Radio Sci.*, *17*, 1425–1433.

Ito, S., T. Oguchi, T. Iguchi, H. Kumagai, and R. Meneghini (1995), Depolarization of radar signals due to multiple scattering in rain, *IEEE Trans. Geosci. Remote Sens.*, *33*, 1057–1062.

Marzano, F. S., L. Roberti, S. Di Michele, A. Mugnai, and A. Tassa (2003), Modeling of apparent radar reflectivity due to convective

clouds at attenuating wavelenghts, *Radio Sci.*, *38*(1), 1002, doi:10.1029/2002RS002613.

Oguchi, T., N. Ishida, and T. Ihara (1994), Effect of multiple scattering on the estimation of rainfall rates using dual-wavelength radar techniques, *IEEE Trans. Geosci. Remote. Sens.*, *32*, 943–946.

Testud, J., P. Amayenc, and M. Marzoug (1992), Rainfall-rate retrieval from a spaceborne radar: Comparison between single-frequency, dual-frequency, and dual-beam techniques, *J. Atmos. Oceanic Technol.*, *9*, 599–623.

Tsang, L., J. A. Kong, and R. T. Shin (1985), *Theory of Microwave Remote Sensing*, Wiley-Interscience, Hoboken, N. J.

M. O. Ajewole, Department of Physics, Federal University of Technology, Akure, Nigeria. (oludareajewole61@yahoo.com)

A. Battaglia and C. Simmer, Meteorological Institute, University of Bonn, Auf dem Hugel, 20, D-53121 Bonn, Germany. (batta@uni-bonn.de)